TRANSIENT THERMAL RESPONSE OF SOLID, PINNED AND HIGHLY POROUS VENTILATED BRAKE DISCS

Timothy Mew

A research report submitted to the Faculty of Engineering and the Built Environment, University of the Witwatersrand, Johannesburg, in partial fulfillment of the requirements for the degree of Master of Science in Engineering.

Johannesburg, 2014

DECLARATION

I declare that this dissertation is my own unaided work. It is being submitted to the Degree of Master of Science to the University of the Witwatersrand, Johannesburg. It has not been submitted before for any degree or examination to any other University.

....

Timothy Mew

This .13th. day of .August.............., .2014.........

ACKNOWLEDGEMENTS

The authors wish to acknowledge the support from SEW-Eurodrive, Alfa International and SKF during the construction of the disc brake testing facility. This research was partially supported by the South Korean Ministry of Education, Science and Technology (MEST) of Korea (Grant number: K2011-0030886) through the International Research & Development NRF Program and through the South African NRF THRIP (Grant number: TP13082630765). Special thanks are extended to Professor K.J. Kang of Chonnam National University in South Korea, for assistance in the fabrication of the highly porous brake disc.

ABSTRACT

During braking, heat is generated due to frictional contact between the brake pads and the brake disc of a vehicle. At elevated temperatures, brake fade may occur, leading to potentially catastrophic brake failure in a vehicle. The heat-dissipating characteristic of a brake disc is a function both of the physical design of the brake disc, and also the brake disc material. This research focuses on the effect of brake disc design, in particular, how the surface temperature is affected by changing the morphology of a brake disc's ventilated channel. The surface temperature of a newly developed brake disc with a wire woven porous ventilated channel (WBD) core (the design of which is not part of this research) was tested and compared to existing commercially available brake discs. The parameters governing the transient thermal response for solid, ventilated, and porous brake discs during extended braking will be identified. The results reveal that the thermal capacity of a brake disc determines the initial rate of brake disc temperature increase (T), resulting in initial temperatures being T(solid disc)$<T$(pin-finned disc)$<T$(WBD disc). However, for extended braking, the ventilated discs run at lower temperatures and reach a lower steady state temperature than the solid rotor: T(solid disc)$>T$(pin-finned disc)$>T$(WBD disc). This is due to the increased convective surface area and addition of forced convection in the ventilated channels. With the porous WBD core, a substantially lower brake disc temperature is achieved.

PUBLISHED WORK

Aspects of this work have been published in the following peer-review conference proceedings:

- T. Mew, T. Kim, K.J. Kang, F.W. Kienhöfer (2013). Transient Thermal Comparison of Solid and Ventilated Brake Discs, 9th South African Conference on Computational and Applied Mechanics, Somerset West, RSA.

This work has also made substantial contributions to the following submitted journal papers:

- H.B. Yan, T. Mew, M-G. Lee, K-J. Kang, T.J. Lu, F.W. Kienhofer, T. Kim (2013). Thermo-Fluidic Characteristics of a Porous Ventilated Brake Disc, ASME Journal of Heat Transfer.

- T. Mew, K.J Kang, F.W. Kienhöfer, T. Kim (2013). Transient thermal response of a highly porous ventilated brake disc, IMechE Part D: Journal of Automobile Engineering (accepted with minor corrections).

CONTENTS **PAGE**

LIST OF FIGURES

LIST OF TABLES

LIST OF SYMBOLS

A_e	effective heat transfer area [m^2]
A_d	surface area of brake disc [m^2]
A_v	surface area in ventilated channel [m^2]
A_s	surface area of shaft [m^2]
C_p	specific heat capacity [J/kgK]
c_1	constant
c_1	constant
d_{WBD}	diameter of helical wire [m]
h_{CE}	external convective heat transfer coefficient on disc surface [W/m^{2}K]
h_{CI}	internal convective heat transfer coefficient on disc surface [W/m^{2}K]
h_S	convective heat transfer coefficient on a shaft [W/m^{2}K]
H_{WBD}	height of WBD unit cell [m]
k	thermal conductivity [W/mK]
l_{h}	helical pitch of WBD wire [m]
L_{WBD}	length of WBD unit cell [m]
M_d	mass of brake disc [kg]
P	input power [W]
t	time [s]
T	brake disc temperature [K]
T_b	torque [Nm]
T_o	ambient (reference) temperature [K]
V	vehicle speed [km/h]
W_{WBD}	width of WBD unit cell [m]
α	gradient [%]
ε	emissivity [-], porosity [-]

1. INTRODUCTION

The braking system converts the kinetic energy of the vehicle into heat, which raises the temperature of the brake disc (or rotor) and pads (Figure 1). Heat build-up occurs at the friction interface during braking. While a certain amount of the heat generated is absorbed by brake components such as the brake caliper by conduction, the majority of heat is absorbed by the disc, which must be effectively cooled to avoid excessive temperatures [1-4].

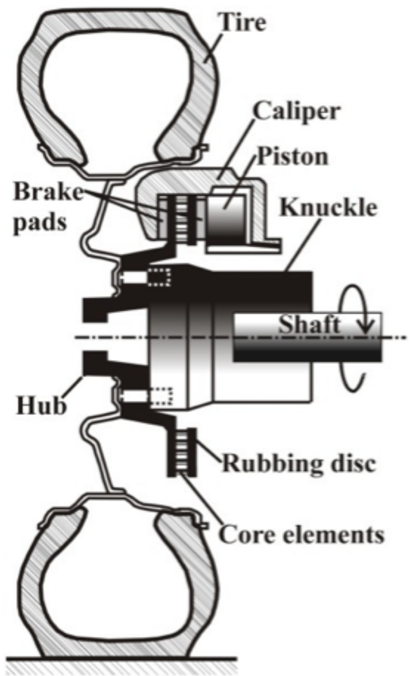

Figure 1. Conventional brake system showing brake disc, pads and caliper.

The braking performance of a vehicle is largely dependent upon the friction coefficient at the brake pad and disc interface. While a moderate temperature rise of a brake disc causes the friction coefficient of brake pads to increase, improve braking performance, elevated operating surface temperatures have a detrimental effect on the disc and the pad wear (illustrated in Figure 2) [5,6]. At elevated temperatures (approximately 550 ºC), the coefficient of friction of the brake pads decreases dramatically, resulting in decreased braking torque performance. This is due to chemical change of the brake pad compound, and the formation of a 'lubrication layer'. Furthermore, the possibility of thermal cracking at these temperatures is increased [7-9].

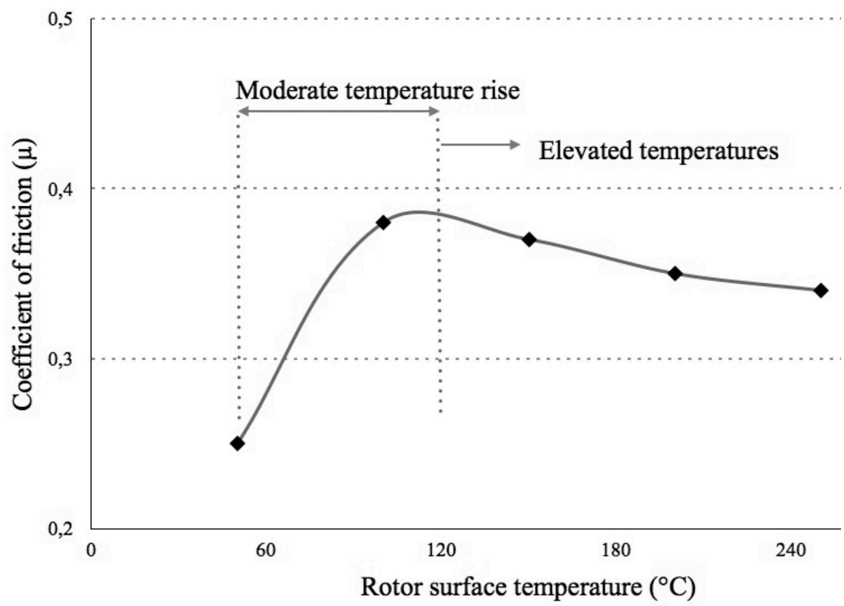

Figure 2. Variation of coefficient of friction with temperature [10]

It is therefore desired to maintain brake surface temperatures within reasonable limits (below 500 ºC), to ensure that the braking system of a vehicle remains fully functional.

Chapter 2 will discuss existing literature concerning heat dissipation in brake discs, and the effect of braking mode on brake temperature. Existing commercially available brake disc designs will also be reviewed for reference.

2. LITERATURE REVIEW

2.1 Brake disc design

Brake discs currently exist in numerous configurations. Examples of these include solid, radially vaned, curved vaned, and pinned rotors (shown in Figure 3). While solid discs possess superior strength and thermal storage capabilities, ventilated discs are able to dissipate heat more effectively, due to convective cooling on both external and internal surfaces.

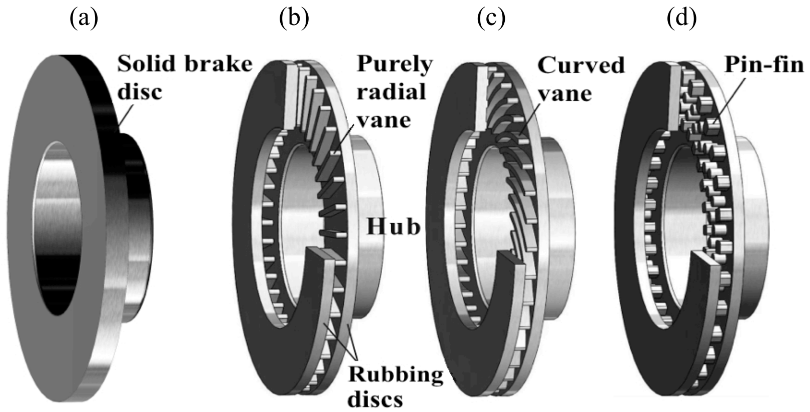

Figure 3. Selected brake disc configurations; (a) Solid disc; (b) Radial vaned disc; (c) Curved-vaned disc; (d) Pin-finned disc.

Daudi et al. [11] highlighted the importance of increasing the rate of the cooling airflow through the ventilated core. To increase the air flowrate through the ventilated core, some brake disk designs use radial vanes (fins, shown in Figure 3) to accelerate the air as the rotor is turning by the centrifugal pumping action of the vanes. Galindo-Lopez et al. [12] used CFD analyses to prove that the heat dissipation through convection could be increased by 14% by placing additional half-length vanes between existing vanes of a standard straight vane rotor. It was concluded that increasing the surface area of the heat exchange core medium resulted in improved convective heat dissipation. Using CFD simulations, Daudi found an optimal radially vaned rotor design, which incorporated 72 radial vanes with an inlet angle of 45 ºC and an exit angle of 105 ºC. A 37% improvement in cooling airflow velocity was achieved in comparison with a standard straight radial vane rotor. Sisson [13] investigated the effect of the number of blades (varying from 20 to 40) on the flow velocity through a radially vaned rotor, and concluded that the number of vanes made little difference to the flow of air. It is evident that additional vanes would not only increase the heat exchange surface area, but also increase the thermal storage capacity of the rotor.

2.2 Heat dissipation

Figure 4 shows a surface temperature comparison of both solid and ventilated rotors heated as a result of frictional brake contact to the same temperature. From the thermal image, the solid rotor displays a relatively uniform surface temperature, while the ventilated disc displays equally spaced hot and cold regions, corresponding to the location of the cooling airflow through the ventilated core. It is evident that a ventilated rotor is able to dissipate heat more effectively through internal cooling channels, compared to a solid rotor.

Heat is removed by conduction through the thickness of the rubbing disc (see Figure 1) from the friction interface to the ventilated core, where it is absorbed into the core elements [14]. The surface area of these elements exposed to the cooling airflow will therefore determine the rate of heat dissipated, and therefore of the rate of heat removed from the friction interface, ultimately reducing the rotor temperature. Furthermore, the rate of conduction increases with an increasing thermal gradient between the external friction interface and the internal cooling channel.

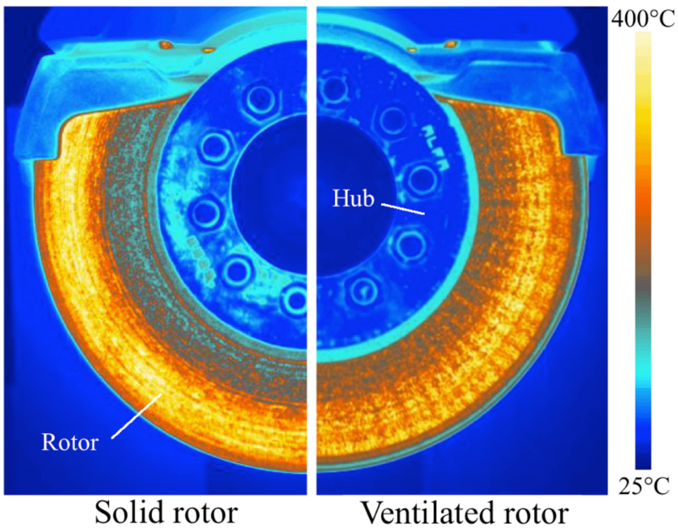

Figure 4. Surface temperature comparison of solid and ventilated brake discs

The cooling capability of a disc is a function of both the design of the brake, and the type of brake application [15-18]. During operation, a vehicle's brake is applied in numerous different braking modes, including continuous, repeated, and single stop braking modes. A particular disc design may have a high cooling capacity for one brake application mode while a relatively poor cooling capacity for a different brake application mode. For a short single brake application, the temperature rise at the friction interface is largely a function of the thermal capacity of the disc, because the rate of heat application generally exceeds the rate of heat dissipation [1]. For this reason, a solid disc (Figure 3a) is expected to operate at a lower temperature during a short brake application in comparison to a ventilated disc (Figure 3b, cored with conventional pin-fins) as a typical solid disc has approximately 30% more mass than a ventilated disc. For longer brake applications, as the temperature of the disc increases, the gradient between the rotor surfaces and the cooling airflow is increased, resulting in a higher rate of heat dissipation via convection. A ventilated disc, therefore, dissipates heat by convection more effectively at elevated temperatures [19-21]. For continuous braking (or extended braking), however, the rate of heat dissipation from the disc will ultimately determine the rotor temperature [22, 24]. As a ventilated disc has larger surface area and convective cooling in the ventilated channel compared to a solid disc, it is capable of dissipating more heat during continuous braking and operating at a lower temperature.

The temperatures of solid and ventilated brake discs are governed by different mechanisms at different braking application modes. A disc will absorb the heat generated at the friction interface until the rate of heat dissipation from the disc is equal to the rate of heat generation, at which point, steady state has been reached. The rate of heat generation can be determined according to the applied braking power [24]. Abbas et al. [25] used numerical methods to show that the convective cooling coefficient of the disc and hub system is the dominant factor influencing the temperature of a disc at steady state. McPhee et al. [26] showed according to classical theory [27, 28] that heat dissipation can be determined empirically in terms of heat storage (conduction) and heat dissipation (convection), but did not investigate the transient thermal influence of a rotor's mass and surface area on rotor surface temperature.

Limpert [19] used a thermal diffusivity term to empirically predict the thermal effect of heat absorption into a disc, while Parker et al. [29] showed that some of the heat generated at the friction interface is dissipated by conduction into the hub and braking components. Therefore, the rate of conduction plays a vital role in determining the heat flux into and from the rotor, and thus the rotor's transient temperature.

The combined effect of heat conduction into the rotor and the corresponding gradual increase in heat dissipation through convection during heating on both initial and final (steady state) rotor temperature has not been fully characterized. The relation between a rotor's mass and convective heat transfer coefficient to transient temperature requires further investigation, including the effect of the increasing temperature gradient between the rotor surface and cooling airflow temperature during braking.

The following chapter will present the research aims of this document, including a hypothesis and problem statement.

3. PURPOSE OF RESEARCH

3.1 Research hypothesis

It is proposed that increasing the surface area of a brake disc's ventilated core will decrease the surface temperature, due to increased heat dissipation by convection. Furthermore, at a constant braking power, the surface temperature of a brake disc will be a function of the brake mode (short braking versus extended braking), and will be determined largely by both the brake disc surface area (convective cooling) and brake disc volume (thermal capacity). A newly developed WBD porous ventilated brake disc will be tested to investigate this theory, and compared to existing commercially available brake discs for reference.

3.2 Problem statement

Chapter 2 presented extensive existing research investigating various brake disc designs and the physical mechanisms of heat dissipation in brake discs, however, little research has been conducted to characterise the parameters affecting the transient brake disc temperature for both short, and extended braking.

With the design of a newly developed highly porous brake disc (not part of this research), it is desired to determine the thermal performance of this brake disc for both short and extended braking, and investigate the parameters that affect the transient thermal behaviour for a constant brake application.

3.3 Research aim

The WBD wire woven porous material is mechanically strong and lightweight, making it a suitable core medium for a new class of brake disc. It is proposed that a wire woven cellular structure would be highly suited as a replacement for conventional ventilated brake disc cores. Such a porous structure would not only significantly increase the surface area exposed to the cooling airflow, but would also increase the rate of airflow through the structure due to the increased porosity. Furthermore, the potential exists for the newly developed highly porous brake disc to induce a more three dimensional airflow, to increase heat dissipation.

A constant brake power will be applied to the brake discs to simulate the extended braking of a vehicle descending a hill, as this is often where brake failure can occur due to brake fade [10].

It is desired in this research to:

1) Measure the transient average surface temperature of a newly developed brake disc for a constant brake application.

2) Compare the temperature of the porous brake disc to existing commercial solid and pin-ventilated brake discs, under identical conditions.

3) Use experimental findings to determine the effect of a rotor's thermal capacity on transient temperature during short braking, and the effect of convective cooling during extended braking.

4) Investigate the effect of increasing the surface area of a rotor's ventilated core on transient surface temperature.

The transient temperature for a specific test case (a set braking power and rotational velocity) will be compared to both solid and ventilated brake discs, a using a purpose built test rig. This will be accomplished using experimental data obtained on a testing rig, and classical theory adopting a first order differential equation approach.

The following chapter will discuss the experimental method used to measure the temperatures of the brake discs, including details of the test rig and equipment used to make the measurements.

4. EXPERIMENTAL DETAILS

4.1 Brake disc testing rig

A test rig was constructed to replicate feasible loads and temperatures experienced by the disc of a medium sized truck during continuous downhill braking. This rig (shown in Figure 6) consists of a 400 V, 37 kW, AC induction motor, with a maximum operating speed of 1500 rpm (1).

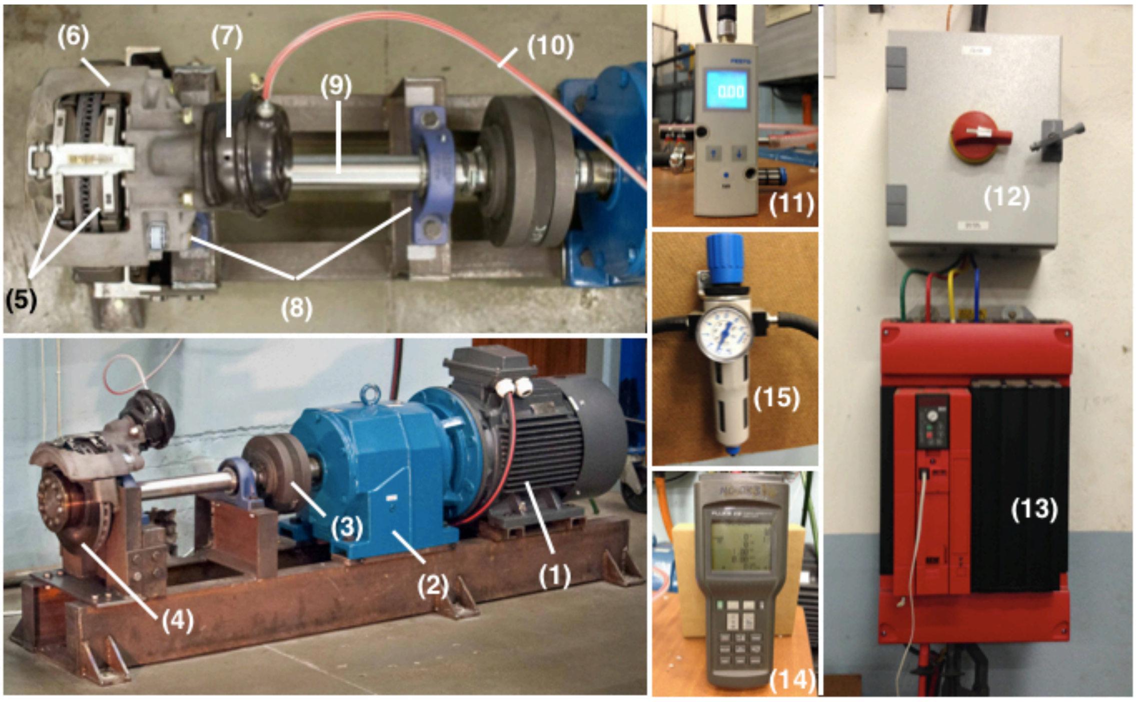

Figure 6. Disc brake testing rig with components

The rotational speed is reduced through a gearbox (2) with a ratio of 3.7:1. A computer controlled frequency inverter (13) regulates the motor speed. The motor is connected to a flexible coupling (3), which transmits the torque to a shaft (9). The shaft has an outer diameter of 60 mm and is manufactured from EN8 mild steel. The shaft rotates on bearings and is flanged at the opposite end to allow the brake discs to be directly attached. A floating brake caliper (6) applies a braking torque to the disc (10) through the actuation of brake pads (5). The brake caliper is actuated using a type 24 pneumatic brake chamber (7), controlled using a digital pressure regulator (11). A tachometer placed on the shaft measures rotational velocity while proprietary software is used to monitor outputs from the thermal camera and frequency inverter. A three-phase power meter (14) is attached directly to the inverter output to measure motor power.

A FLIR T640 thermal camera was used to capture and record the brake surface temperature change over time. The specifications of this camera are listed in Table 1.

Table 1. FLIR T640 infra-red thermal camera specifications [31]

Temperature range	-40 to 150 °C
	100 to 650 °C
	650 °C to 2000°C
Spectral range	7.8 to 14 μm
Image frequency	30 Hz
Accuracy	+/- 2 °C
Emissivity correction	0.1 to 1.0

4.2 Experimental procedure

To simulate a truck descending at a constant speed down a constant hill decline, it was required to ensure that the rotor speed and braking power were kept constant. This was accomplished by constantly compensating the brake pressure to maintain the desired braking power (displayed on the power meter).

The test procedure is described below:

1) Ensure brake disc and all braking components are at room temperature, and brake is completely released.
2) Turn on motor, and set the desired rotational velocity.
3) Set the emissivity of the thermal camera to the calibrated value of the brake disc, and commence recording on the thermal camera software.
4) Increase brake pressure rapidly until desired braking power is displayed on the power meter.
5) Adjust brake pressure as necessary to compensate for changing coefficient of friction of the brake pads as the temperature rises, to ensure that brake power remains constant for the entire length of the test.

6) When the desired time is completed or the rate of temperature increase has slowed to a satisfactory level (indicating steady state), stop recording.
7) Release brake, and turn off motor.

4.3 Thermal camera calibration

To obtain surface temperatures of brake discs, an infrared camera (FLIR T640) was used. To accurately measure the disc surface temperatures using infrared (IR) thermography, it is essential to determine the emissivity for each brake disc. This was accomplished by operating the brake disc for a sufficient period of time to raise the temperature of the disc to well above ambient conditions (to approximately 200 ºC), after which the true temperature was determined. A calibrated T-type thermocouple was mounted on the surface of the disc when stationary, and the emissivity of the IR thermal camera was compensated until its temperature reading correlated with the thermocouple reading. This was repeated at three different locations on each brake disc to ensure measurement accuracy.

The emissivity of the brake discs was found to be $\varepsilon = 0.79$ (for the solid disc), $\varepsilon = 0.74$ (for the pin-finned disc), and $\varepsilon = 0.80$ (for the porous disc). The temperature measurement area of the thermal camera is shown as region A in Figure 7. The average temperature was measured at a frequency of 30 Hz, and recorded for post processing. The emissivity calibration process was repeated every 4-5 tests, to check if the gradual colour change of the brake disc had affected the emissivity.

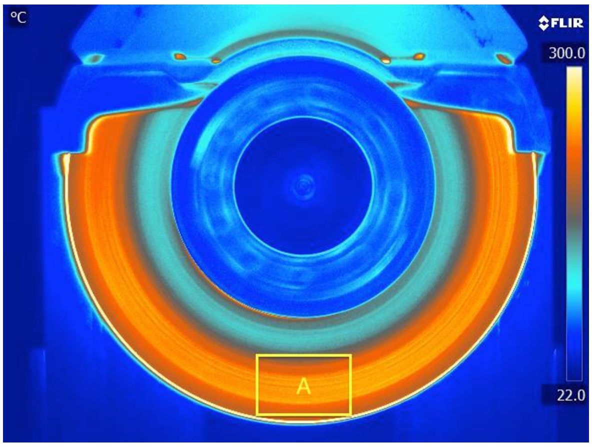

Figure 7. Thermal camera temperature measurement area (region A).

4.4 Solid and pin-finned brake discs

Three brake discs (a solid disc, a ventilated discs cored with pin-fins, and a highly porous WBD brake disc) were tested. A commercially available solid brake disc made of grey cast iron was selected (Figure 8a and 4a). A pin-finned brake disc made of grey cast iron was also tested (Figures 8d, 4b), containing four rows of pin-fin elements sandwiched between two rubbing discs. The two central rows of the pin-fins have a circular cross-section whilst the innermost and outermost rows of pin-fins have a blunt end. In total, 120 pin-fins are arranged with 30 pin-fins in each row. The pin-fins occupy approximately 30% of the total volume of the ventilated channel, resulting in a porosity of approximately 0.7 and a surface area density of approximately 81 m^2/m^3.

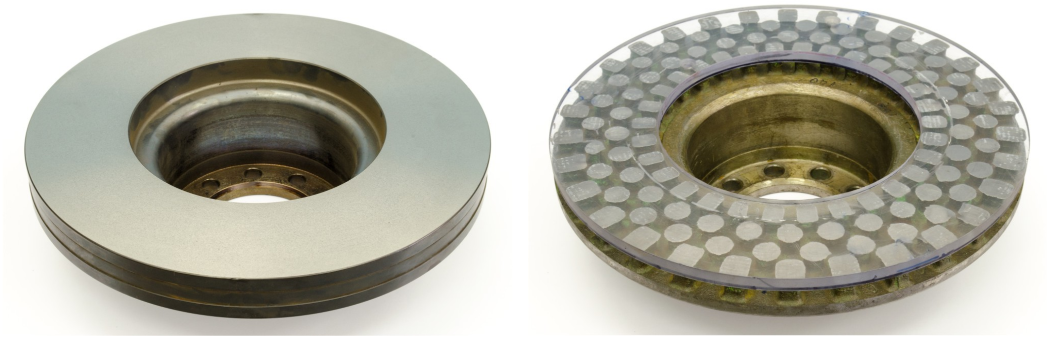

a) b)

Figure 8. Tested brake discs having one transparent rubbing disc for displaying a core medium; (a) Solid disc; (b) Pin-finned disc.

4.5 A porous brake disc with wire-woven bulk diamond (WBD) core

Various periodic cellular materials with tetrahedral, pyramidal, and Kagome unit cells have been recently developed [34-36]. Studies have shown that such materials have excellent specific strength/stiffness, as well as heat dissipation capability [37-40], making them a good candidate material for lightweight ventilated brake discs where high thermal and mechanical load bearing capabilities are required. In this study, a ventilated brake disc with a wire-woven bulk diamond (WBD) core is integrated into the ventilated channel of a brake disc (Figure 9a).

The annular WBD core is fabricated using cold-rolled mild steel helical wires with a diameter of d_{WBD} = 1.5 mm and a helical pitch of l_{h} = 19.0 mm. The assembly is brazed at 1120 °C in a de-oxidation atmosphere of H_2N_2 mixture [34,35]. The unit cell of the WBD core (shown in Figure 9) is composed of two types of ligaments: ligament II has twice the length of ligament I. The overall dimensions of the unit cell are: $L_{WBD} = 9.5$ mm, $W_{WBD} = 9.5$ mm, and $H_{WBD} = 14.0$ mm. The porosity and surface area density of the WBD core are ~0.9 and ~255 m^2/m^3 [21].

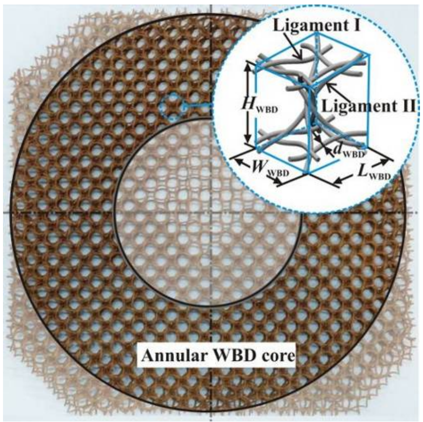

a)

b)

Figure 9. Wire-woven bulk diamond (WBD) showing an annular WBD core and its unit cell (a) [35], with one transparent rubbing disc used to display the core medium (b).

The equivalent yield strength, maximum strength, and Young's modulus of the core are 3.2 MPa, 4.8 MPa, and 1.08 GPa, respectively [21]. The outer diameter, disc thickness and hub dimensions of the WBD brake disc are identical to those of both the pin-finned and solid brake discs. The specific heat, mass and thermal conductivity values for the three discs considered in this research are listed in Table 2.

Table 2. Physical properties of the brake discs [29,30].

Brake disc type	Properties
Solid brake disc	- Grey cast iron
	- C_p = 505 J/kgK
	- M_d = 18.67 kg
	- k = 47.8 W/mK
Pin-finned ventilated brake disc	- Grey cast iron
	- C_p =505 J/kgK
	- M_d = 14.22 kg
	- k = 47.8 W/mK

WBD porous ventilated brake disc	- Mild steel
	- C_p = 473 J/kgK
	- M_d = 13.47 kg
	- k = 43 W/mK

4.6 Simulated conditions

The brake power P is related to the vehicle velocity V and hill inclination α in the following equation:

$$P = Mg\sin(\alpha)V \tag{3}$$

Test parameters were set to simulate a vehicle of a fixed mass descending a hill gradient α with speed V km/h. A perfectly balanced brake distribution is assumed, as illustrated in Figure 10. Each brake disc retards an effective mass of M/n kg with braking force F_b N per wheel where n is the number of wheels. For V = 40 km/h, the disc's rotational speed is set at 200 rpm, leading to P = 1.9 kW, T_b = 89 Nm and α = 2.0% for M/n = 900 kg.

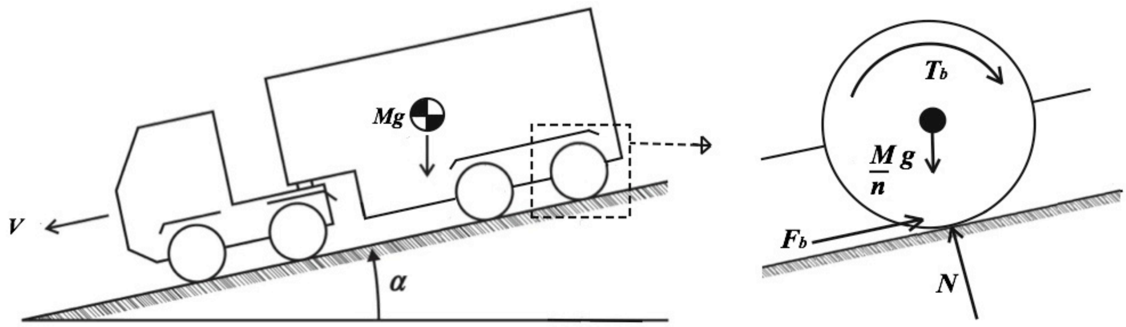

Figure 10. Force balance of a truck with the total mass of M, descending a hill.

4.7 Measurement uncertainty analysis

The uncertainty of the disc rotational speed was estimated to be less than 5 rpm. The FLUKE™ 43B power meter has an accuracy of 1%, yielding maximum power reading deviations of approximately 20 W. The FESTO digital pressure regulator has an accuracy of ±0.005 bar, and is programmable in steps of 0.01 bar.

Ambient air temperature was measured by a calibrated T-type thermocouple (Omega) with a resolution of 0.1 ºC. During each test, the fluctuation of ambient temperature was measured to be within ±0.4 ºC. The temperature measured by the infrared camera showed a deviation of ±0.2 ºC from that measured by the foil type thermocouple (Omega). The accuracy of the thermal camera is specified as ±2 ºC in the temperature range used (100 to 600 ºC), with a resolution of 1 ºC. Due to misalignment of the rotor and imperfect contact of the brake pads with the rotor, the temperature fluctuation across the surface of the rotor was measured to deviate by ±5 ºC.

4.8 Theoretical analysis

The heat transfer from the friction interface of a brake disc is largely due to conduction into the brake disc (Q_C) and surrounding brake components, but also due to convection into the cooling airflow around the brake disc (Q_V). At elevated temperatures (exceeding 400 °C), heat transfer by radiation (Q_R) becomes increasingly dominant. The components are listed below:

$$Q_C = kA_r \Delta T_r / \Delta x \tag{4}$$

$$Q_V = h_r A_r (T_r - T_\infty) \tag{5}$$

$$Q_R = \varepsilon \sigma A_r (T_r^4 - T_\infty^4) \tag{6}$$

The heat stored in a brake disc may be expressed as:

$$Q_D = M_D C_P \frac{dT}{dt} \tag{7}$$

It is assumed for simplicity that heat is only stored in the brake disc and the shaft (representing the braking components, see Figure 6). Heat dissipation from the shaft may be represented by the classical fin equation [27], with the assumption of a prescribed tip temperature:

$$Q_S = \sqrt{hpkA_S}\,\vartheta_b \frac{\cosh(mL) - (\vartheta_L - \vartheta_b)}{\sinh(mL)} \tag{8}$$

where:

$$\vartheta_b = T_b - T_\infty$$

$$\vartheta_L = T_L - T_\infty$$

$$m = \sqrt{\frac{hp}{kA_s}}$$

A_s, p and h are the surface area, perimeter and convective heat transfer coefficient of the shaft respectively. Equation (8) may be represented more conveniently:

$$Q_S = \frac{\sqrt{h_S p k A_S}}{\tanh\left(\sqrt{h_S p / (k A_S)}\right)}\left(T(t) - T_O\right) \tag{9}$$

To account for the differing heat transfer coefficients for the external and internal (ventilated core) rotor surfaces, two effective convective heat transfer coefficients are defined: h_{CE} and h_{CI}. It is convenient to combine both the radiation and convection components to give a combined rotor heat dissipation term:

$$Q_V = \left((h_{CE} + h_R)A_{CE} + h_V A_V\right)\left(T(t) - T_o\right) \tag{10}$$

An energy balance for a single rotor absorbing a power P generated as heat due to friction may be expressed by:

$$P = Q_V + Q_S + Q_D \tag{11}$$

A brake disc mounted to a shaft of diameter d is shown in Figure 10, depicting the energy balance detailed in equation 11.

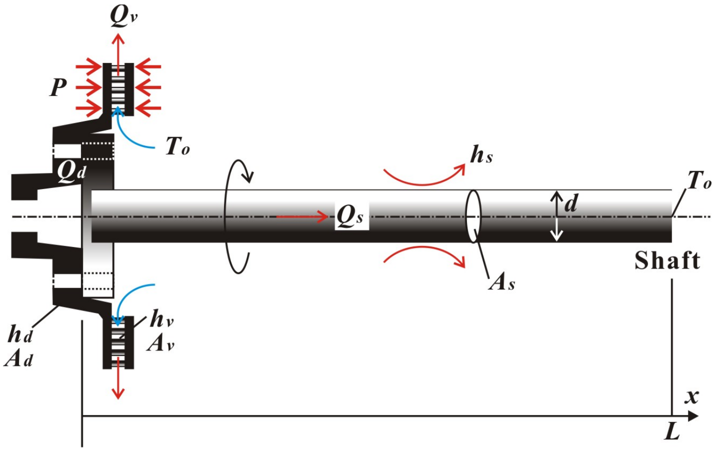

Figure 10. Schematic representation of energy balance in a brake system.

The first two terms of equation 11 give:

$$Q_V + Q_S = \left((h_{CE} + h_R)A_{CE} + h_{CI}A_{CI}\right)\left(\frac{\sqrt{h_S pkA_S}}{\tanh\left(\sqrt{h_S p/(kA_S)}\right)}\right)\left(T(t) - T_O\right) \tag{12}$$

Which may be simplified by defining:

$$c_1 = \left((h_{CE} + h_R)A_{CE} + h_{CI}A_{CI}\right) + \frac{\sqrt{h_s pkA_s}}{\tanh\left(\sqrt{h_s p/(kA_s)}\right)} \tag{13}$$

The third term of equation 11 may be simplified by defining:

$$c_2 = M_D C_P \tag{14}$$

At steady state, the heat dissipation by convection is given by (5). To isolate the governing parameters that characterize transient behaviour, an effective heat transfer coefficient and area are defined for steady state: $h_E A_E = c_1$. Now, from (5), it is known that convective heat dissipation at steady state is given by:

$$h_E A_E = \frac{P}{\left(T(t) - T_O\right)} = c_1 \quad (15)$$

Finally,

The energy balance conducted in (11) may now be represented in the simple form:

$$P = c_2 \frac{d\theta}{dt} + c_1 \theta \quad (16)$$

The general solution of equation 16 may then be given by:

$$\theta(t) = Ce^{-(c_1/c_2)t} + \frac{P}{c_1} \quad (17)$$

Since the boundary conditions at t = 0 are known, it is calculated that $C = -P/c_1$ at $\theta(t)$=0. Combining this result with (16), the temperature increase of the brake disc as a lumped mass with time may be expressed as:

$$\theta(t) = \frac{P}{c_1}\left(1 - e^{-(c_1/c_2)t}\right) \quad (18)$$

Differentiation of equation 18 would yield the gradient (rate) of the temperature increase:

$$\frac{d\theta}{dt}(t = 0) = \frac{P}{c_2} \quad (19)$$

Furthermore, at steady state ($t = \infty$), it can be shown from equation 18 that the steady state temperature is given by:

$$\theta(t=\infty)=\frac{P}{c_1}=\frac{P}{h_E A_E} \tag{20}$$

From equation 19 therefore, it is shown that the rate of increase of temperature is inversely proportional to the thermal capacity ($c_2 = C_P M_D$), and that the rate of increase is independent of the effective heat transfer coefficient and area $h_E A_E$.

From equation 20, it is shown that the steady state brake disc temperature is independent of both the effective heat transfer coefficient and area, and the brake disc thermal capacity.

While the braking power P is an independent variable, constants c_1 and c_2 need to be determined for a set power. A brake power of P = 1.9 kW is considered in this case. From the specific heat, thermal conductivity and mass of each brake disc listed in Table 3, c_1 and c_2 may be calculated from equations 14 and 15 respectively.

Table 3. Measured and calculated brake disc parameters.

Brake disc configuration	Parameters
Solid disc P = 1.9 kW	- $c_1 = c_p m_d$ = 9428 J/K - $c_2 = h_E A_E$= 5.6 W/K - $\theta_\infty = T_\infty - T_o$ = 339.0 K
Pin-finned disc P = 1.9 kW	- $c_1 = c_p m_d$ = 7181 J/K - $c_2 = h_E A_E$ = 6.6 W/K - $\theta_\infty = T_\infty - T_o$ = 290.0 K
Porous disc P = 1.9 kW	- $c_1 = c_p m_d$ = 6371 J/K - $c_2 = h_E A_E$ = 7.5 W/K - $\theta_\infty = T_\infty - T_o$ = 253.0 K

This chapter has reviewed the theoretical brake disc temperature increase for both transient and steady state conditions. Chapter 5 will discuss these results in relation to the experimental data obtained from the three brake discs tested, and will investigate the effect that these parameters have on transient brake temperature.

5 RESULTS

To characterise and compare the transient thermal performance for constant downhill braking (in this case, specifically for a medium sized truck), three brake disc configurations were considered, namely, solid, pin-ventilated, and porous WBD. These discs were tested at a braking power of 1.9 kW, and a rotational speed of 200 rpm (40 km/h for a medium sized truck). Figure 8 compares the disc surface temperature distribution of the solid (Figure 8a), pin-finned (Figure 8b) and porous (WBD, Figure 8c) discs at selected intervals captured by a pre-calibrated thermal camera.

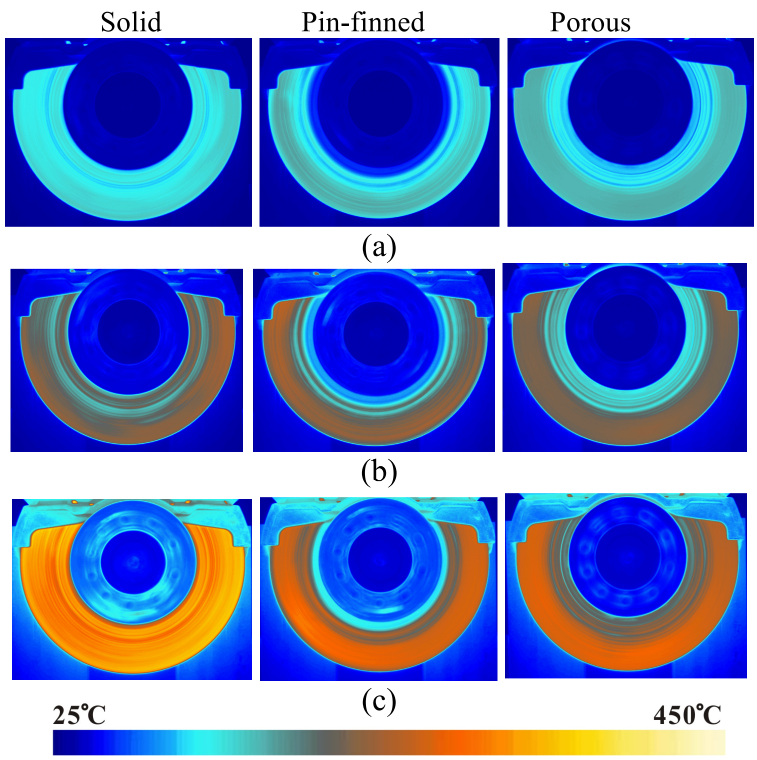

Figure 8. Comparison of transient cooling performance of three brake discs, simulating 2% gradient continuous downhill braking at a vehicle speed of 40 km/h (200 rpm) and a braking power of 1.9 kW; (a) at $t = 850$ s; (b) $t = 1600$ s; (c) $t = 5500$ s.

Figure 9a shows the recorded surface temperatures of the three brake discs, tested at a power of 1.9 kW, and a rotational speed of 202 rpm. Three regions are defined from this result:

1. Region (a) – initial temperature rise (short braking)
2. Region (b) – cross-over point
3. Region (c) – steady state temperature (extended braking).

The smooth circumferential distribution of the surface temperature on the rubbing discs indicates a good contact between the brake pad and discs, shown in Figure 9b. There exists a radial variation of the surface temperature since the brake pad is in contact with the rubbing disc radially from 0.76*r/R* to 1.0*r/R*, where *R* is the outer radius of the brake disc.

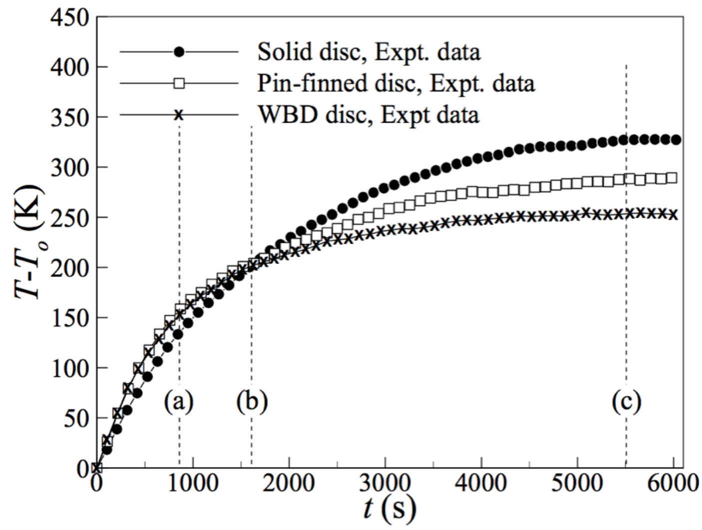

(a)

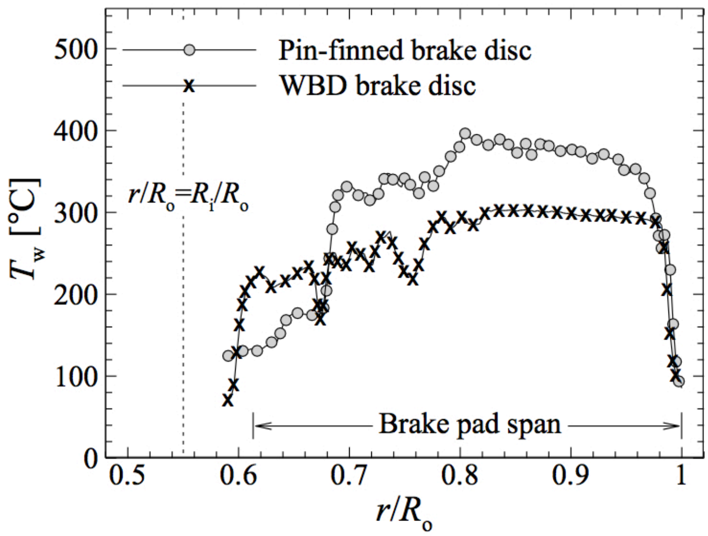

(b)

Figure 9. Temporal variation of average disc surface temperature of a solid disc, ventilated discs cored with pin-fins and WBD, where average disc temperature differences (T-T_o) at steady state are T(Solid) = 327.0K, T(pin-ventilated) = 289.4K, and T(WBD) = 253.0K (a), radial temperature profile of both discs at steady state (b).

Figure 10 depicts the theoretical temperature rise for constant brake application, using the parameters calculated in Table 2, and relations derived in section 4.8. In Figure 10a, $h_E A_E$ is fixed at the calculated value of 5.6 W/K, while the effective thermal capacity $C_P M_D$ is increased from 5000 J/K to 15000 J/K. Figure 10b depicts the temperature rise for a fixed effective thermal capacity, while $h_E A_E$ is increased from 5.6 W/K to 10W/K.

These figures graphically depict the impact of thermal capacity and convective cooling respectively, and are discussed in section 6.

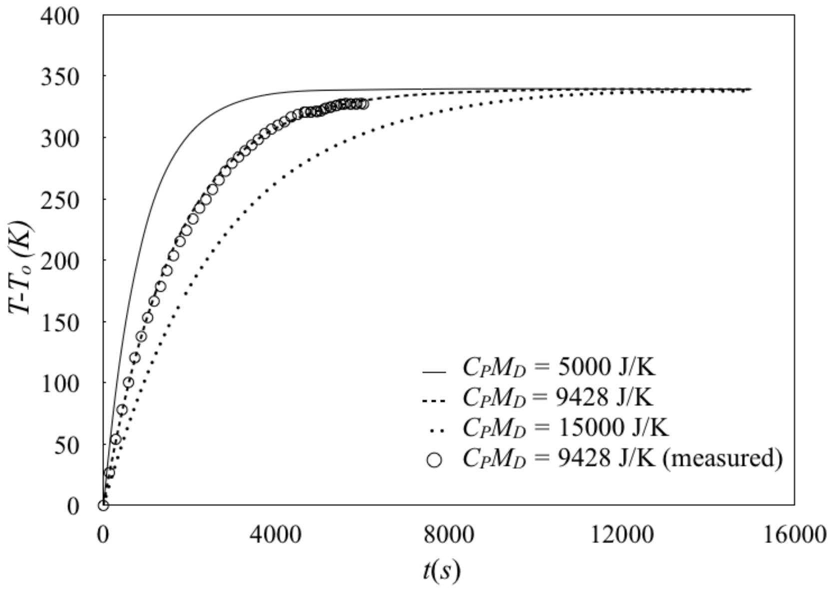

(a)

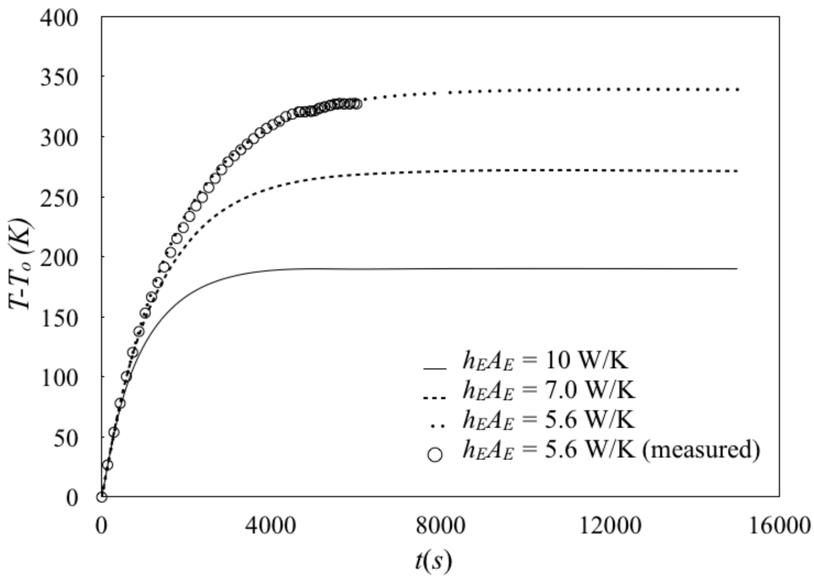

(b)

Figure 10. Effect of rotor thermal capacity C_PM_D (a), and convective rotor cooling h_EA_E (b) on the average brake disc surface temperature, including experimental data of the solid disc.

This chapter has presented the experimental results obtained in this study. The following chapter will present an explanation of these results in relation to brake disc thermal capacity, and convective cooling.

6. DISCUSSION

Figure 9a shows the results of the average surface temperature (indicated by region A in Figure 7), recorded at the conditions detailed in section 5. Three phases are identified during the heating of the rotors: (a) initial, (b) crossover, and (c) steady state. As soon as braking is initiated, the surface temperature of the three brake discs steeply increases (a). The rate of increase gradually decreases however, finally reaching a steady state temperature (c), the magnitude of which depends on the configuration of the brake disc. From Figure 9a, at t = 850 s, it is clear that the surface temperature of the WBD and pin-finned brake discs is higher than that of the solid disc: 16% for the pin-ventilated disc, and 13% for the WBD disc. After further braking, both the pin-ventilated and WBD brake discs maintained a lower surface temperature than the solid brake disc.

During short braking, both ventilated brake discs show slightly higher disc temperatures, passing a crossover point (b) where their disc temperatures are the same as that of the solid disc. After which, the pin-finned and WBD discs provide superior cooling performance to the solid disc. At steady state (c), the average disc temperature of the pin-finned disc is approximately 12% lower than that of the solid disc whilst the WBD brake disc exhibits approximately 23% lower surface temperature than the solid disc: T(Solid)>T(Pin-fin)>T(WBD).

It has been observed that initially, the average surface temperature of the ventilated brake discs (pin-finned and porous discs) increases more rapidly than that of the solid disc i.e., T(Solid)>T(Pin-fin)>T(WBD) but begins to approach steady state temperatures earlier, which are substantially lower than that of the solid disc. As a combined result of the two, there is a crossover indicated as (b) in Figure 9a. The higher thermal capacity of the solid brake disc therefore, results in a lower surface temperature for short braking, as the rotor is able to absorb more heat in comparison to a ventilated rotor. The greater surface area due to the inner ventilated channel of the ventilated brake disc results in superior cooling, particularly at elevated temperatures, as the rate of heat dissipation rises with an increasing thermal gradient between the rotor surface and cooling airflow. Therefore, the forced convective cooling in the ventilated brake disc results in a lower steady state temperature being attained. The WBD disc results in a lower steady state temperature in comparison to the pin-finned disc, due to a greater surface area in the ventilated core.

The following chapter will present conclusions drawn from the results of the experimental and theoretical findings.

7. CONCLUSIONS

It was desired to compare the transient thermal response of a newly developed highly porous brake disc with that of existing commercially available solid and pin-ventilated discs. The test condition simulated a typical heavy vehicle downhill descent at 40 km/h (corresponding to a disc rotational velocity of 202 rpm), generating a braking power of 1.9 kW per brake disc. Shortly after the brake are applied, the ventilated discs show slightly higher disc temperatures (see Figure 9a), but after extended braking, the ventilated discs run at lower temperatures, indicating that the thermal performance of a brake disc is dependent upon the brake mode, and braking time.

The WBD wire woven porous material is mechanically strong and lightweight, making it a suitable core medium for a new class of brake discs. The integration of this porous medium into a ventilated brake disc core reduces the overall weight of the brake disc (24% lighter than the solid brake disc, and 5% lighter than the pin-ventilated brake disc). Studies [40,41] have shown that a weight reduction improves fuel efficiency (particularly for vehicles with multiple axles), by reducing the driven vehicle load. A lightweight disc is of particular benefit to high performance vehicles requiring lightweight wheels, possessing a low rotational inertia, allowing for more rapid acceleration and deceleration. Furthermore, the disc weight impacts the un-sprung weight of all vehicles. A lightweight disc improves suspension performance, as the vertical inertia transmitted through the shock absorber and damper to the chassis is reduced when driving on uneven road surfaces.

It was proposed in the research hypothesis that increasing the surface area of the ventilated core will decrease the brake disc surface temperature, due to increased heat dissipation by convection. The results of this report have confirmed this, with experimental and theoretical temperature responses indicating lower steady state temperatures of the newly developed WBD brake disc, compared to both the solid and conventional pin-ventilated discs. The transient thermal behavior of brake discs is influenced primarily by the disc material specific heat, mass, and surface area exposed to a cooling airflow. Therefore, while a lightweight disc may typically have a greater exposed surface area, the reduced weight has a negative impact on the brake disc temperature at the initial braking period (or during short braking). However, during extended braking, as experimentally demonstrated in this study, a porous core substantially enhances internal cooling in the ventilated channel, leading to a lower overall operating disc temperature compared with the conventional pin-finned brake disc (approximately 14%) and the solid brake disc (approximately 23%).

The conclusions drawn from the findings in this report are summarized below.

(1) It was shown using classical first order differential equations that the thermal capacity ($C_P M_D$) of a brake disc dramatically affects the rate of temperature increase for short braking (shown in Figure 10a). A disc with a high thermal capacity is able to absorb and store more heat by conduction, reducing the temperature at the friction interface.

(2) Similarly, it was shown using differential equations, that the effective convective cooling heat transfer coefficient and surface area ($h_E A_E$) influences the steady state temperature of a brake disc. From Figure 10b, it is shown that a brake disc with $h_E A_E$ = 10 W/K yielded a steady state temperature of approximately 160 ºC lower than a disc with an effective convective cooling term of 5.6 W/K.

(3) During short braking ($0<t<1500$ s), the solid disc runs at a lower temperature, due to larger thermal capacity. The reduced mass for ventilated brake discs resulting from the ventilation causes higher brake disc temperature.

(4) During extended braking ($t>1500$ s), the internal cooling in the ventilated channel reduces the brake disc temperature substantially. Although the temperature of the ventilated brake disc increases sharply during the initial braking period, it runs at a lower steady state temperature.

(5) The temperature of the porous disc increases sharply during short braking (even more so than the pin-finned disc due to a lower thermal capacity). The increased surface area of the ventilated core flow mixing promoted by the three-dimensional WBD's morphology leads to a substantially lower overall disc temperature at steady state.

The aim of this research was to measure the transient thermal behaviour of a newly developed brake disc, and determine governing parameters affecting immediate temperature rise, and steady state temperature. This has been accomplished using a brake disc test rig to compare the temperatures of the three brake discs considered in this report. It has been demonstrated using classical first order equations that a rotor's thermal capacity has the greatest influence on immediate temperature rise, while the convective cooling capability of a brake disc will determine the maximum temperature experienced for a specific braking event.

This research has further shown that although the newly developed porous brake disc is able to dissipate heat more effectively during extended braking, the tested solid and ventilated brake discs run at lower temperatures for rapid, or short braking. Although the rate of the increase in the disc temperature was steeper than the solid and fin-pinned brake discs during short braking, the WBD brake disc settled to a lower steady state temperature during extended braking.

8. RECOMMENDATIONS

This research has investigated and compared the transient thermal response of a new highly porous brake disc. The results show that an increased brake disc thermal capacity reduces brake temperature during short braking (due to increased immediate heat absorption by conduction). It is therefore recommended that the ventilated core of the new highly porous brake disc be modified to increase thermal capacity, while maintaining a large surface area. This could be accomplished by incorporating elements of existing ventilated brake discs (such as pins or fins) into the wire woven core of the porous brake disc, essentially forming a hybrid design.

Research investigating and comparing various configurations for a range of braking powers and rotational speeds would allow for an optimal brake disc design to be formulated, and targeted at a specific class of vehicle.

9. REFERENCES

1. A. Day. The dissipation of frictional energy from the interface of an annular brake disc. Proceedings of the Institution of Mechanical Engineers, Part D: J. Automobile Engineering. (11)198-201, 1984.
2. R. Limpert. Cooling analysis of brake disc rotors. SAE Paper 751014, 1975.
3. S. Bernsteiner, D. Wallner. Friction Force Measurement at Brake Discs. SAE Paper, 2011-01-1576, 2011.
4. D. Antanatis, J. Sanford. The effect of racetrack / High energy driving on brake caliper performance. SAE Paper 2006-01-0472, 2006.
5. M. Liu, The relationship between friction interface and pad wear. SAE Paper 2012-01-1792, 2012.
6. R. Eisengraber, J. Grochowicz, M. Schuster, "Comparison of Different Methods for the Determination of the Friction Temperature of Disc Brakes." SAE Paper 1999-01-0138, 1999.
7. M. Duzgun. Investigation of thermo-structural behaviors of different ventilation applications on brake discs. Journal of Mechanical Science and Technology. 26(1) 235-240, 2012.
8. T.J. Mackin, S.C. Noe et al. Thermal cracking in disc brakes. Engineering failure analysis, Permagon, 9(63-76), 2002.
9. T. Okamura, H. Yumoto. Fundamental study on thermal behaviour of brake discs. SAE Paper 2006-01-3203, 2001.
10. A. Ilm, P. Leung, P.K Datta. Experimental investigations of disc brake friction. SAE paper 2000-01-2778, 2000.
11. A. Daudi, H. Lemmerz. Hayes high airflow design rotor for improved thermal cooling and coning. SAE paper 982248, 1998.
12. C.H. Galundo-Lopez, M. Tirovic. Understanding and improving the convective cooling of brake discs with radial vanes. Proceedings of the Institution of Mechanical Engineers, Part D: J. Automobile Engineering, 222(7), 1211-1229, 2008.

13. A.E. Sisson. Thermal analysis of vented brake rotors. SAE paper 780352, 1978.
14. R. Limpert. Brake Design and Safety, SAE International, Third Edition, Warrendale, PA, USA, 2011.
15. D.B. Antanaitis. Engineered surface features for brake discs to improve performance in fade conditions. SAE Paper 2013-01-2039, 2013.
16. G.P. Ostermeyer, M. Muller, H. Abendroth, B. Wernitz. Surface topography and wear dynamics of brake pads. SAE Paper 2006-01-3202, 2006.
17. O.O. Evtushenko, Y.O. Pyr'ev. Temperature and wear of the friction surfaces of a cermet patch and metal disk in the process of braking. Materials Science, 36(218-224), 2000.
18. A. Apte, H. Ravi. FE Prediction of Thermal Performance and Stresses in a Disc Brake System. SAE Paper 2006-01-3558, 2006.
19. R. Limpert. The thermal performance of automotive disc brakes. SAE Paper 750873, 1975.
20. B. Nutwell, T. Ramsay. Modeling the cooling characteristics of a disk brake on an inertia dynamometer, using combined fluid flow and thermal simulation. SAE Paper 2009-01-0861, 2009.
21. P. Hwang, X. Wu, Y. Jeon. Repeated brake temperature analysis of ventilated brake disc on the downhill road. SAE Paper 2008-01-2571, 2008.
22. A. Adamowicz, P. Grzes. Influence of convective cooling on a disc brake temperature distribution during repetitive braking. Journal of applied thermal engineering. 31(2177-2185), 2011.
23. F. Talati, S. Jalalifar. Analysis of heat conduction in a disc brake system, Heat and Mass Transfer. SAE Paper, 45(8), 1047-1059, 2009.
24. Y. Huang, S. Chen. Analytical study of design parameters on cooling performance of a brake disk. SAE Paper 2006-01-0692, 2006.
25. S.A. Abbas, N.J. Cubitt, C.J. Hooke. Temperature Distributions in Disc Brakes. Proceedings of the Institution of Mechanical Engineers: Automobile Division, 184(185-194), 1969.
26. A.D. McPhee, D.A. Johnson. Experimental heat transfer and flow analysis of a vented brake rotor. International Journal of Thermal Sciences, 47(458-467), 2008.

27. M.J. Moran, H.N. Shapiro. Fundamentals of engineering thermodynamics, 6th Edition. USA, 2008.
28. F.P. Incropera, D.P Dewitt. Fundamentals of heat and mass transfer. 4th Edition, Toronto, Canada, 1996.
29. Alfa Brakes, Material Properties Catalogue, cast iron technical specifications, online: www.alfabrakes.co.za/layout_images/technical%20specifications.pdf, last accessed 20 February 2014.
30. POSCO Mill Test Certificate, Certificate no: 090413-KHNE-172-001, POSCO Gwanyang Works, Jeolianam-do, Korea; May, 2012.
31. Information obtained from www.flir.com, last accessed 7 Aug 2014.
32. G.P. Voller, M. Tirovic, R. Morris, P. Gibbens. Analysis of automotive disc brake cooling characteristics. Proceedings of the Institution of Mechanical Engineers, Part D: J. Automobile Engineering, 217(8) 657-666, 2003.
33. F. Highley. Techniques for determining the thermal characteristics of brake drums and discs. SAE Paper 710589, 1971.
34. R.C. Parker, T.P. Newcomb. The performance and characteristics of the disc brake. SAE Paper 836A, 1964.
35. H.N.G. Wadley, Multifunctional periodic cellular metals, Philosophical Transactions of the Royal Society A: Mathematical, Physical and Engineering Sciences, 364(1838) 31-68, 2006.
36. Y.H. Lee, B.K. Lee, I. Jeon, K.J. Kang, Wire-woven bulk Kagome truss cores, Acta Materialia, 55(18) 6084-6094, 2007.
37. M.G. Lee, G.D. Ko, J. Song, K.J. Kang, Compressive characteristics of a wire-woven cellular metal, Materials Science and Engineering: A, (539) 185-193, 2012.
38. T. Kim, C.Y. Zhao, T.J. Lu, H.P. Hodson, Convective heat dissipation with lattice-frame materials, Mechanics of Materials, 36(8) 767-780, 2004.
39. J.H. Joo, K.J. Kang, T. Kim, T.J. Lu, Forced convective heat transfer in all metallic wire-woven bulk Kagome sandwich panels, International Journal of Heat and Mass Transfer, 54(25) 5658-5662, 2011.
40. S.S. Feng, M.Z. Li, J.H. Joo, K.-J. Kang, T. Kim, T.J. Lu, Thermomechanical properties of brazed wire-woven bulk kagome cellular metals for multifunctional applications, Journal of Thermophysics and Heat Transfer, 26(1)66-74, 2012.

41. T. Fu, D. Cebon. Economic evaluation and the design of vehicle suspensions. International Journal of Vehicle Design. 31(2125-161), 2003.
42. W.J. Midgley, D. Cebon. Comparison of regenerative braking technologies for heavy goods vehicles in urban environments. Proceedings of the Institution of Mechanical Engineers: Automobile Division. 226(7) 957–970, 2012.